Phytopathology Research

RESEARCH

Open Access

FpOGT is required for fungal growth, stress response, and virulence of *Fusarium proliferatum* by affecting the expression of glucokinase and other glucose metabolism-related genes

Yizhou Gao[1], Yitong Wang[1], Siming He[1], Haibo Li[1], Yuqing Wang[1] and Zhihong Wu[1*]

Abstract

O-GlcNAcylation, an important post-translational modification catalyzed by O-GlcNAc transferase (OGT), plays critical roles in several biological processes. In this study, we present our findings on the function of FpOGT in regulating physiological processes and pathogenicity of *Fusarium proliferatum* (*Fp*), the alfalfa root rot fungus. The deletion of *FpOGT* impaired mycelial growth and altered macroconidia morphology in *Fp*. Furthermore, Δ*FpOGT* mutant displayed altered tolerance to various stressors, including cell wall perturbing agents, osmotic stressors, metal ionic stressors, and fungicides. Deletion of *FpOGT* significantly decreased *Fp* virulence toward alfalfa. The transcriptome analysis demonstrated that FpOGT plays a regulatory role in glucose metabolic pathways, including glycolysis, tricarboxylic acid (TCA) cycle, and hexosamine biosynthesis pathway (HBP), by influencing the expression of relevant genes. The downregulation of the glucokinase gene, *FpGCK*, was observed in Δ*FpOGT*, and the disruption of *FpGCK* led to a decrease in *Fp* virulence. Additionally, FpOGT affected the expression levels of the *FpGCK*-AS1 isoform, thereby impacting glucokinase function. The molecular docking analysis elucidated the plausible physical interaction between FpOGT and FpGCK, thereby offering valuable insights into their interrelationship. These findings underscore the indispensable involvement of FpOGT, the sole O-GlcNAc transferase in *Fp*, in various biological processes and the pathogenicity through its regulation of fundamental metabolic processes. Consequently, this study emphasizes the significance and elucidates the molecular mechanism underlying the role of O-GlcNAc transferase in diverse fundamental biological processes and the pathogenicity of phytopathogenic fungi.

Keywords *Fusarium proliferatum*, FpOGT, Glucokinase, Glucose metabolism, Virulence, Alfalfa

Background

Alfalfa (*Medicago sativa*), a highly nutritious leguminous forage, represents a critical protein feed source and is extensively cultivated (Dang and Li 2022). Alfalfa root rot arises due to the infection of diverse soil-borne fungi, with *Pythium* spp., *Fusarium* spp., and *Rhizoctonia solani* taking center stage as predominant and commonly isolated pathogens of significant concern (Berg et al. 2017; Yang et al. 2023). The complexes of pathogens collaborate to form alfalfa root rot, rendering the search for a host-resistant genotype a big challenge (Abbas et al. 2022). Fungicidal treatments and cultivation measures represent the primary approaches to managing the root rot disease, while the implementation of biological control agents remains sparsely documented (Abbas et al. 2022). *Fusarium proliferatum* (*Fp*) was identified as a new pathogen

*Correspondence:
Zhihong Wu
wulab_zust@163.com
[1] School of Biological and Chemical Engineering, Zhejiang University of Science and Technology, Hangzhou 310023, China

causing alfalfa root rot in China (Cong et al. 2016). *Fp* can also infect a variety of economically important plants, leading to losses in crop yield and quality with contamination by mycotoxins, including fumonisins, beauvericin, moniliformin, fusaproliferin, fusaric acid, and bikaverin posing a severe threat to food safety (Sun et al. 2019; Lalak-Kanczugowska et al. 2023). The control measures against the new pathogen *Fp* on alfalfa remain unresolved, and the understanding of its pathogenic mechanisms may provide a theoretical foundation critical for developing effective disease management strategies.

Protein O-GlcNAcylation is a common post-translational modification found in multicellular eukaryotes, involving the attachment of β-linked N-acetylglucosamine to serine and threonine residues of proteins (Chatham et al. 2021). The process is catalyzed by O-GlcNAc transferase (OGT) using uridine diphosphate N-acetylglucosamine (UDP-GlcNAc) as the donor substrate, which is derived from the hexosamine biosynthetic pathway (HBP), making O-GlcNAcylation responsive to nutrient availability (King et al. 2019; Hu et al. 2021). Importantly, this modification is reversible, facilitated by the presence of the O-GlcNAcase (OGA), which efficiently removes O-GlcNAc modifications (Joiner et al. 2019). This reversibility allows for dynamic cycling and responsiveness to environmental stresses (Fahie et al. 2022). The impact of O-GlcNAcylation on proteins is multifaceted, influencing protein function, interactions with other proteins, cellular localization, and stability (Ma et al. 2021). Additionally, O-GlcNAcylation can interplay with other post-translational modifications (PTMs), including phosphorylation, ubiquitinylation, sumoylation, and acetylation, acting as a molecular switch in response to nutrient status and stress (Hart et al. 2011). In conclusion, protein O-GlcNAcylation is a crucial nutrient and stress-responsive modification that plays diverse roles in cellular processes through dynamic cycling and crosstalk with other PTMs (Yang and Qian 2017).

The biological function of O-GlcNAcylation has been extensively studied in various species. In plants, O-GlcNAc modification plays a role in hormone response, development, and stress response (Olszewski et al. 2010; Xu et al. 2019). Tomato O-GlcNAc transferase SlSEC1 enhances SlC3H39 O-GlcNAcylation and contributes to its function in cold tolerance (Xu et al. 2023a). O-GlcNAcylation also regulates histone lysine methyltransferase activity, influencing epigenetic processes, and its modification of *Arabidopsis* DELLA protein RGA has been linked to the regulation of multiple signaling activities during plant development (Zentella et al. 2016; Xing et al. 2018; Mutanwad and Lucyshyn 2022). Beyond plants, O-GlcNAcylation is also implicated in human diseases, including neurodegenerative disorders, diabetes, and cancers, affecting macrophage inflammatory and antiviral responses (Machacek et al. 2018; Lee et al. 2021). Studies involving *OGT* knockout in mice have provided insights into its significance in multiple immune cell functions (Chang et al. 2020). Moreover, in *Caenorhabditis elegans*, the absence of OGT increases sensitivity to the infection of the human pathogen *Staphylococcus aureus* (Bond et al. 2014), while in *Drosophila*, O-GlcNAcylation is crucial for developmental regulation, stem cell maintenance, circadian rhythm, and responses to ambient temperature (Mariappa et al. 2018; Na et al. 2022). In conclusion, O-GlcNAcylation stands as a fundamental regulatory mechanism in diverse cellular processes, contributing to a multitude of critical biological functions in different species. Nevertheless, functional investigations of OGT in fungi, particularly concerning its role in the pathogenicity of plant pathogenic fungi, remain notably scarce.

Glucokinase (GCK), a member of the hexokinase family, plays a key role in glucose metabolism by facilitating the conversion of glucose to glucose-6-phosphate, initiating the first step of glycolysis (De Backer et al. 2016). Glucokinase has distinctive biochemical properties that give it specialized capabilities as a glucose-sensing enzyme (Ren et al. 2022). In addition, research has demonstrated the involvement of glucokinase in glucose signaling in yeast, plants, and mammals (Kim et al. 2006; Kriegel et al. 2016; Sternisha and Miller 2019). In *Saccharomyces cerevisiae*, three enzymes are responsible for hexose phosphorylation: Hxk1, Hxk2, and Glk1 (Bergdahl et al. 2013). While each of these enzymes can support growth in the presence of glucose, the presence of at least one of the two hexokinases is essential for growth when fructose is the primary energy source (Bergdahl et al. 2013). Remarkably, in mouse liver, glucokinase undergoes O-GlcNAcylation, a modification that determines its stability and regulatory functions (Baldini et al. 2016). Glucose-induced O-GlcNAcylation regulates its expression, further highlighting its intricate role in maintaining glucose homeostasis (Tan et al. 2021). However, the O-GlcNAcylation of GCK and its regulatory mechanism in nutrient sensing are not well understood.

This study involved a thorough bioinformatic analysis of the OGT protein in 38 fungal species. We successfully validated the role of FpOGT in the development, pathogenicity, and stress responses in *Fp*, such as growth, spore morphogenesis, response to abiotic stresses, and resistance to fungicides. Moreover, we have elucidated the impact of FpOGT on the expression of *FpGCK*-AS1 alternative splicing isoform, thereby affecting glucokinase activity and regulating various biological processes.

Results

Identification and phylogenetic analysis of OGT proteins in fungi

We identified a putative O-GlcNAc transferase gene (*FPRO_11883*) through BLASTp searching in the *Fp* genome database and named the sole gene *FpOGT*. Gene annotation reveals that *FpOGT* contains four introns, and the entire coding sequence is 4476 bp, encoding a 1491 amino acid protein. To further analyze the conservation of OGT proteins in fungi, we used HMMER search tool to identify the proteins containing the Glyco_transf_41 domain (Pfam ID: PF13844) among 48 fungi protein databases and identified 38 putative OGT proteins (Additional file 1: Table S1). Notably, OGT was not identified in *Saccharomyces cerevisiae, Candida albicans*, and *Cryptococcus neoformans*, and other reports also mentioned the lack of OGT in yeast (Nakanishi et al. 2017; Li et al. 2021). Subsequently, these 38 OGT sequences were used to construct a neighbor-joining phylogenetic tree. As shown in Fig. 1a, the predicted OGTs are clustered into the *Ascomycota* and *Basidiomycota* groups. All OGT members contain two highly conserved Glyco_transf_41 and tetratricopeptide repeat (TPR) domains. The TPR domain is responsible for protein-protein interactions (D'Andrea and Regan 2003). According to their lifestyles and nutrition acquisition strategies, these 38 fungi were classified as animal pathogens, biotrophic fungi, hemibiotrophic fungi, necrotrophic fungi, and saprotrophic fungi. Violin plots were generated to illustrate the distribution of protein lengths (Fig. 1b) and isoelectric points (Fig. 1c) for each category of fungi. We also identified five conserved motifs in OGT proteins using the MEME motif search tool (Additional file 2: Figure S1). These results indicated that the OGT proteins are partly conserved in different fungi. To get more insights into the structural features of OGT proteins, secondary structure and tertiary structure models of OGT proteins were predicted and analyzed for *F. fujikuroi*, *F. graminearum*, *F. oxysporum*, *F. proliferatum*, *F. solani*, and *F. verticillioides*. The results demonstrated a high similarity in the secondary structure, with almost identical proportions of α-helices, β-sheets, β-turns, and random coils (Additional file 2: Figure S2a). The tertiary structure models also indicated a high similarity among OGT proteins (Additional file 2: Figure S2b, c), suggesting significant conservation of OGT protein structures within the *Fusarium* spp.

FpOGT regulates the hyphal growth and macroconidial morphology

To investigate the role of *FpOGT*, we employed the homologous recombination technique to create single-gene deletion mutants (Additional file 2: Figure S3a). Through PCR analysis using gene-specific primers (Additional file 1: Table S2), three deletion transformants were obtained (Additional file 2: Figure S3b). The replacement of *FpOGT* with a single copy of the *HPH* (hygromycin phosphotransferase gene) cassette was confirmed by Southern blotting (Additional file 2: Figure S3c). Moreover, the expression levels of *FpOGT* were undetectable in the deletion mutants (Additional file 2: Figure S3e). We attempted to complement the Δ*FpOGT* strain but could not clone the full length of the *FpOGT* gene from the genomic DNA or cDNA. Therefore, the mutant was complemented with the truncated FpOGT (Δ*FpOGT*-TV-C), which contained two TPR and two Glyco_transf_41 domains (Fig. 2a). The complemented strains were confirmed by PCR and qPCR analysis (Additional file 2: Figure S3d, e). We observed that the *FpOGT* expression was elevated on nutrient-rich media, potato dextrose agar (PDA), but comparatively lower on nutrient-poor media, minimal medium (MM). Additionally, we analyzed the relative expression of *FpOGT* during the infection process on alfalfa seedlings. We found that the expression level was significantly lower than that in mycelia of PDA cultures, indicating that *FpOGT* was expressed at a higher level under conditions of ample nutrient availability (Fig. 2b).

The growth rates of wild-type (WT), Δ*FpOGT,* and the complemented Δ*FpOGT*-TV-C strains cultivated on PDA were subsequently measured to investigate the involvement of FpOGT in hyphae growth. We observed that Δ*FpOGT* exhibited a reduced hyphal growth on PDA (~21%) compared to WT (Fig. 2c and Additional file 2: Figure S4d), while there was no significant difference in the number of macroconidia produced by Δ*FpOGT* and WT (Fig. 2d). The hyphae growth of Δ*FpOGT*-TV-C strain was partially restored, but not to the levels of WT (Fig. 2c). The hyphae growth of ectopic transformants showed no significant difference with WT (Additional file 2: Figure S4d). Further examination of the morphology revealed that 52% of macroconidia produced by Δ*FpOGT* were in the range of 20–40 μm, whereas only 37% of WT macroconidia fell within this size range (Fig. 2e). These findings suggest that FpOGT plays crucial roles in both vegetative growth and macroconidia morphology in *Fp*.

FpOGT is involved in response to different environmental stresses

The maintenance of normal hyphal morphology and environmental stress resilience in fungi is heavily dependent on cell wall integrity (Huang et al. 2023). To investigate the impact of FpOGT on cell wall integrity, we measured the growth rate of Δ*FpOGT* and WT strains on PDA supplemented with cell wall perturbing agents Congo Red (CR), Calcofluor White (CFW),

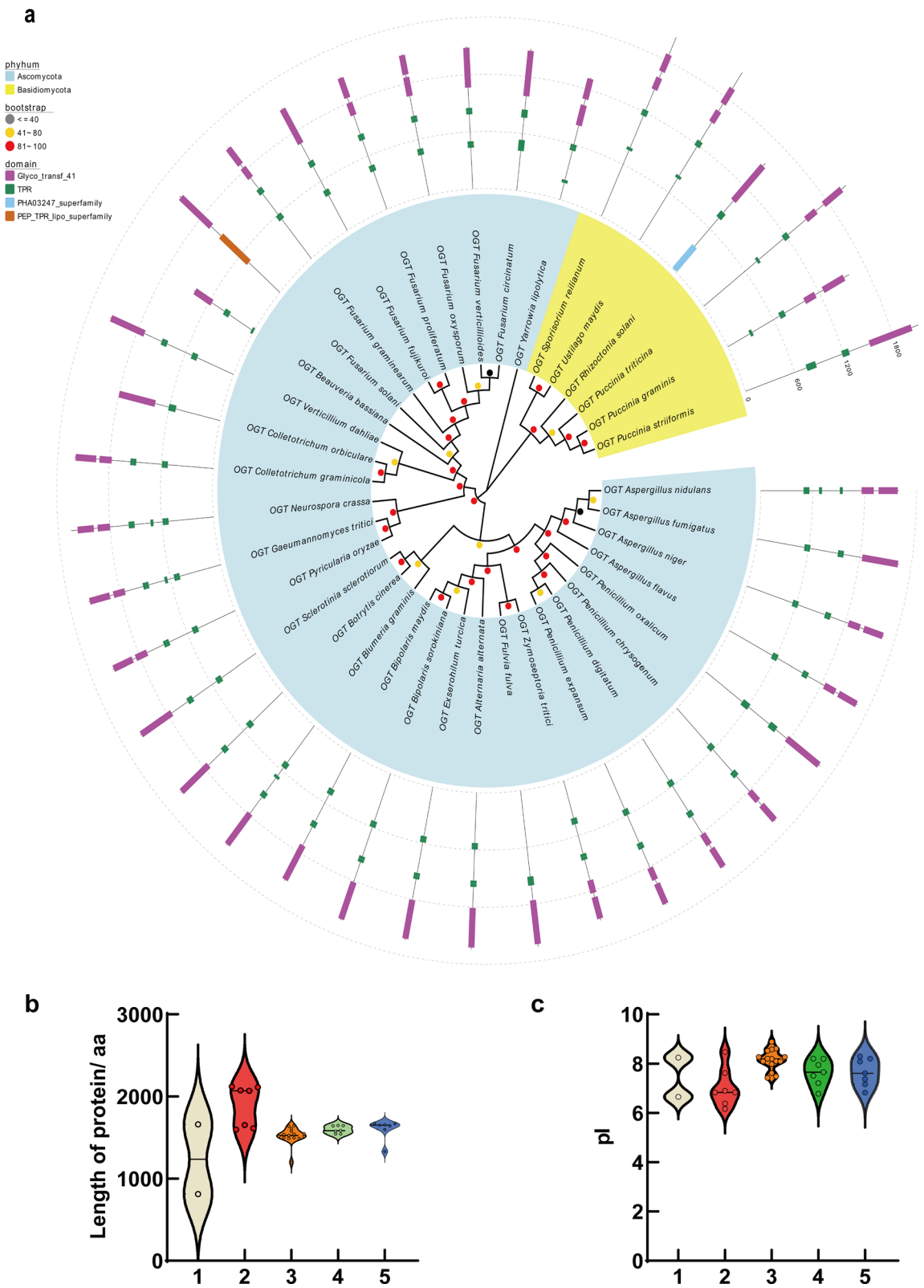

Fig. 1 Phylogenetic tree and physicochemical properties of fungal OGT proteins. **a** Phylogenetic tree and conserved domains of OGTs in fungi. **b** Violin plot of protein length statistics. **c** Violin plot of protein isoelectric point statistics. 1, Animal pathogen; 2, Biotroph; 3, Hemibiotroph; 4, Necrotroph; and 5, Saprotroph

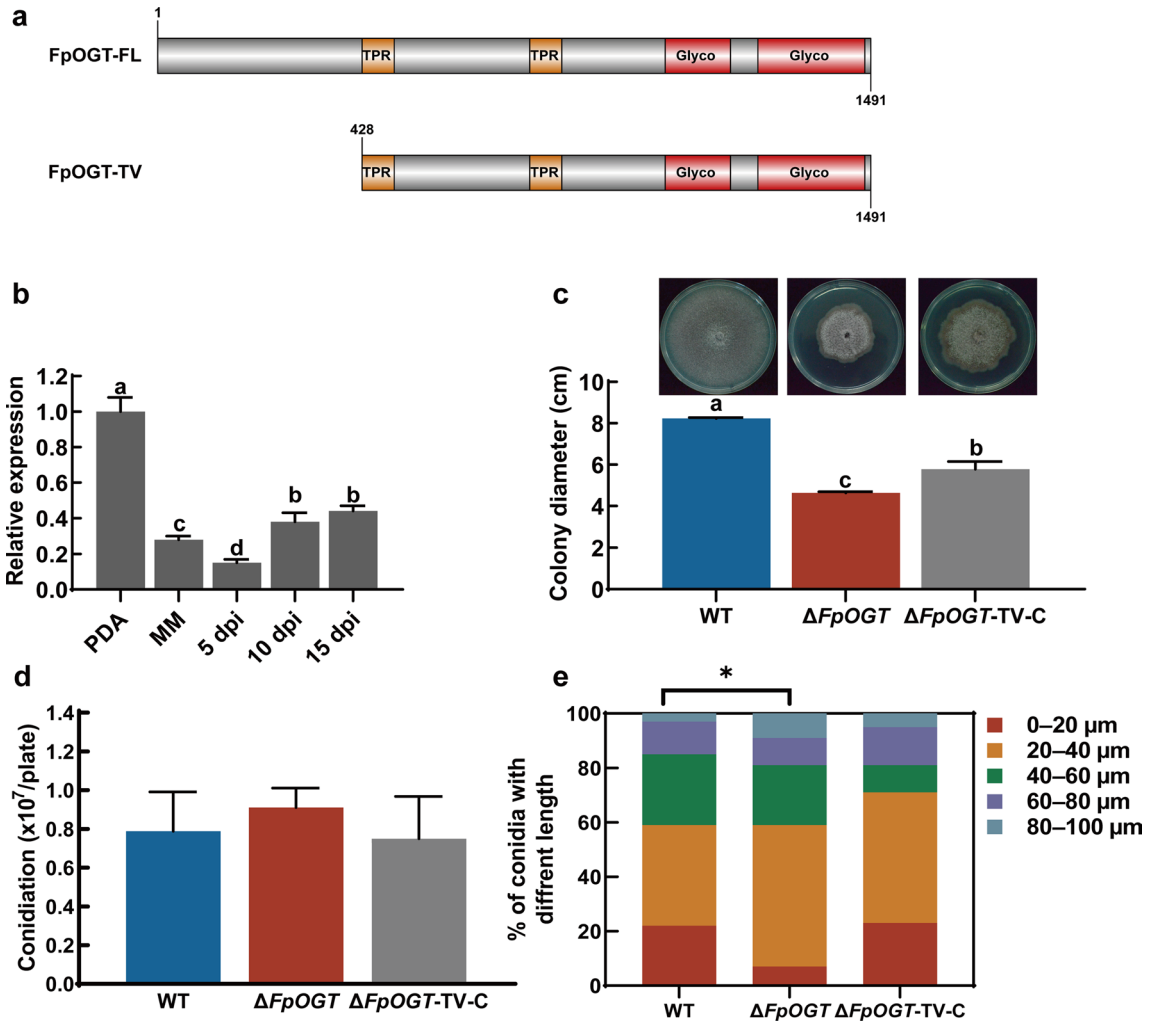

Fig. 2 Role of *FpOGT* in fungal growth and development. **a** Conserved domains of the full-length (FpOGT-FL) and the truncated version (FpOGT-TV) of proteins. **b** Relative expression levels of *FpOGT* in media and *in planta*. Alfalfa seedlings were inoculated by WT strain using the culture plate method. The infected alfalfa seedlings were collected at 5, 10 and 15 dpi as *in planta* samples. RT-qPCR data was normalized against the transcript level of *FpActin*. **c** Colony morphology and colony diameters of the WT, Δ*FpOGT*, and Δ*FpOGT*-TV-C on PDA plates at 28 °C at 7 d. **d** Conidiation capacity of the WT, Δ*FpOGT*, and Δ*FpOGT*-TV-C. **e** Macroconidial length of the WT, Δ*FpOGT*, and Δ*FpOGT*-TV-C. Error bars represent standard deviation, and asterisks indicate a significant difference (*t*-test, $^*P < 0.05$)

and Sodium dodecyl sulfate (SDS). We found that the growth inhibition rates of Δ*FpOGT* were significantly lower than those of WT (Fig. 3a, b). However, the growth inhibition rate of Δ*FpOGT* was markedly higher than that of the WT strain when cultivated on plates supplemented with NaCl (Fig. 3a, b), suggesting that Δ*FpOGT* was more sensitive to osmotic stress. Conversely, Δ*FpOGT* was more resistant to $CaCl_2$-induced metal ionic stress (Fig. 3a, b). The sensitivity tests with the chosen commercial fungicides demonstrated that Δ*FpOGT* exhibited enhanced resistance to chlorothalonil and metalaxyl but increased sensitivity towards *Bacillus subtilis* and fludioxonil (Fig. 3c, d). These findings indicate that FpOGT may regulate the response of *Fp* to diverse environmental stresses.

FpOGT is required for full virulence in *Fp*

The involvement of FpOGT in pathogenicity was evaluated by plate inoculation of mycelia on alfalfa seeds. Ten days after inoculation, wilting and yellowing symptoms caused by *Fp* appeared on seeds or seedlings, and the disease severity of alfalfa seedlings was classified into four grades. We observed that the disease severity of 38% of the Δ*FpOGT*-inoculated seedlings was grade 0, and 44% was grade 1; in contrast, 67% of the WT-inoculated seedlings were classified as grade 3 (Fig. 4a, b).

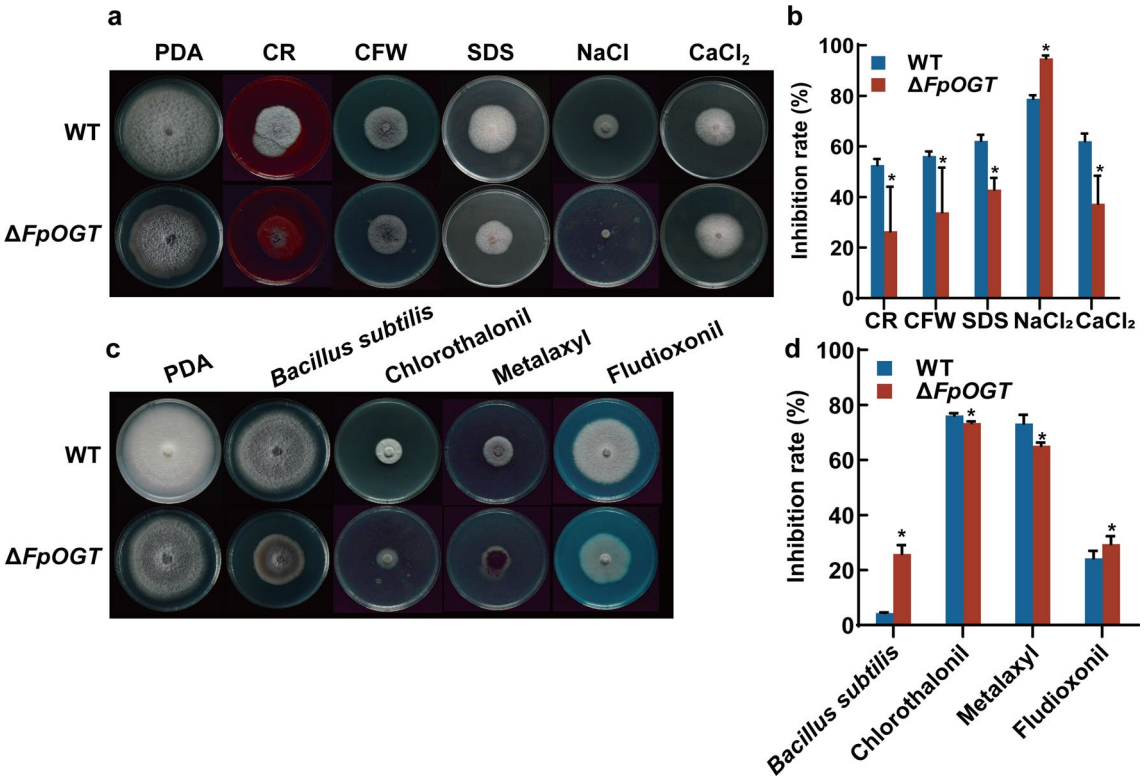

Fig. 3 FpOGT is required for stress and fungicide tolerance. **a** and **b** Colony morphology and Inhibition rates of *Fp* strains on media containing 0.2% CR, 0.2% CFW, 0.05% SDS, 2 M NaCl, 1.4 M $CaCl_2$. **c** and **d** Colony morphology and Inhibition rates of *Fp* strains under treatment of 0.2% *Bacillus subtilis*, 0.05% chlorothalonil, 0.05% metalaxyl, 0.2% fludioxonil. Asterisks indicate the level of statistical significance (*t*-test, $^*P < 0.05$)

The disease index of the Δ*FpOGT*-inoculated seedlings was significantly lower than that of the WT-inoculated plants (Fig. 4c). We observed that the disease index of the Δ*FpOGT*-TV-C-inoculated seedlings was partially restored to about 75% of the WT level (Fig. 4c). Subsequently, we examined the disease progression within 30 days post-inoculation and found that Δ*FpOGT*-inoculated alfalfa seedlings exhibited delayed symptom development and disease progress compared to the WT-inoculated seedlings (Fig. 4d, e).

The other two *FpOGT* knockout transformants, Δ*FpOGT*-2 and Δ*FpOGT*-3, and an ectopic transformant were also tested for virulence. Results revealed that *FpOGT* knockout mutants exhibited reduced virulence, while the ectopic transformant showed no obvious change in virulence compared to the WT (Additional file 2: Figure S4a–c). To further investigate the growth of Δ*FpOGT in planta*, we assessed the relative fungal biomass within the tissues of inoculated seedlings by qPCR using *FpITS* as an indicator and alfalfa *MsRBL* as an internal reference. Results showed that the relative fungal growth of Δ*FpOGT* was markedly lower than that observed in plants inoculated with WT (Fig. 4f), indicating that *FpOGT* is required for full virulence of *Fp.*

FpOGT modulates the expression of genes involved in RNA metabolism, ribosome metabolism, and pathogenic process

To comprehend the molecular mechanism underlying the *FpOGT*-mediated biological processes, we performed RNA-seq analysis to evaluate global changes in gene expression. The cultures of WT and Δ*FpOGT* strains grown in PDB at 28°C for 3 d were collected for RNA-seq analysis. A total of 1402 differentially expressed genes (DEGs) were identified, among which 310 DEGs were upregulated and 1092 DEGs were downregulated in Δ*FpOGT* when compared to WT ($|\text{Fold change}| \geq 2$ and $\text{padj} < 0.05$) (Fig. 5a). Based on Gene Ontology (GO) enrichment analyses, DEGs were enriched in processes such as ribonucleoprotein complex biogenesis, ribosome biogenesis, ncRNA processing, rRNA processing, ribonucleoprotein complex, rRNA metabolic process, and structural constituent of ribosome (Fig. 5b). The DEGs were subsequently screened within the PHI-base (Pathogen-host interactions database), employing a rigorous PHI identity threshold surpassing 60%. A comprehensive screening revealed 24 genes, precisely categorized as reduced virulence genes, comprising 16 up-regulated genes and eight down-regulated genes (Additional file 1:

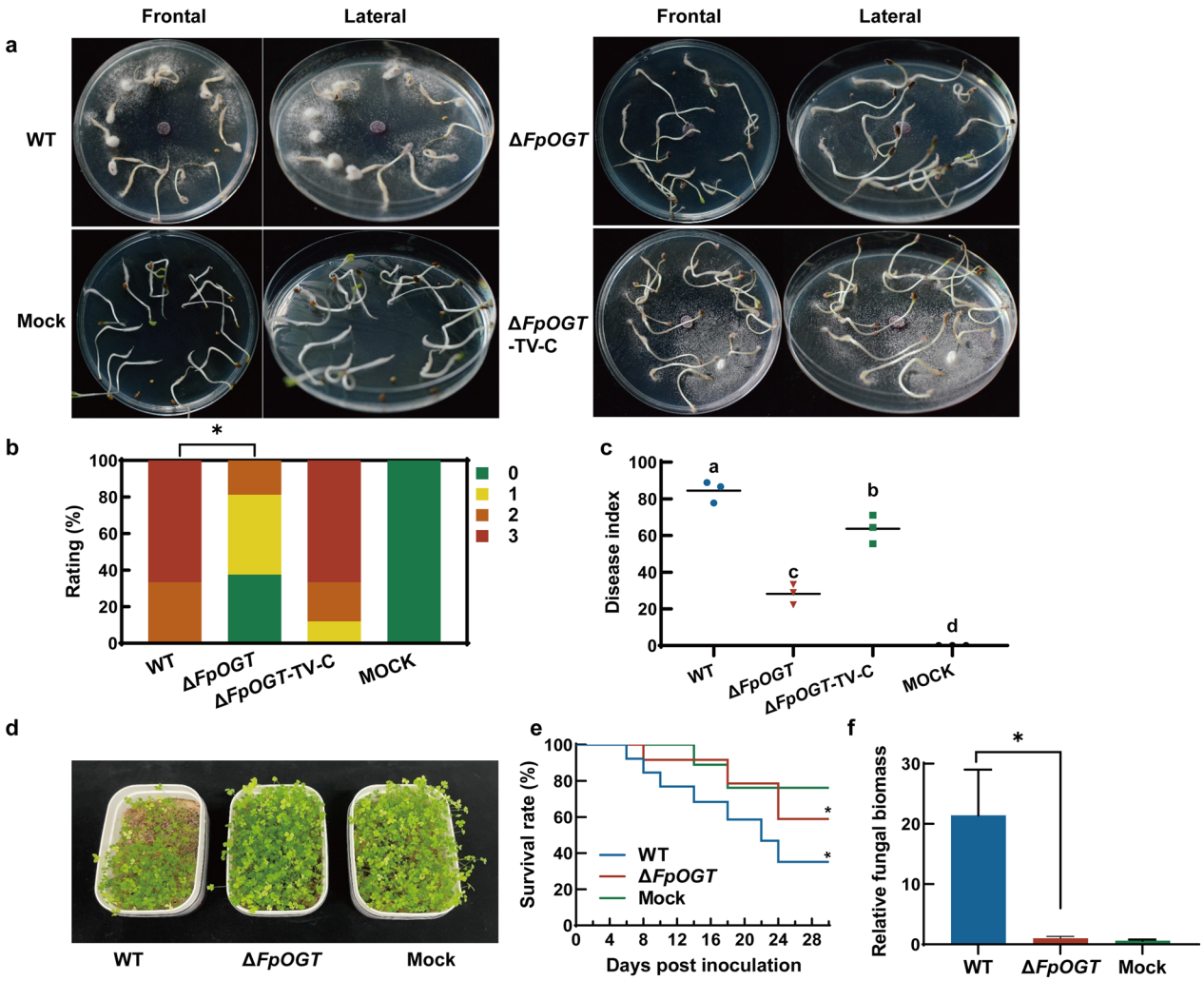

Fig. 4 FpOGT is required for the virulence of *Fp* on alfalfa. **a** Disease phenotype, **b** Disease rating percentages, and **c** Disease index of seedlings inoculated with the WT-, Δ*FpOGT*-, and Δ*FpOGT*-TV-C strains at 10 dpi. **d** Symptoms of alfalfa plants inoculated with the WT and Δ*FpOGT*. **e** Survival curves of the WT, Δ*FpOGT*-inoculated plants during a 30 days experimental period. These experiments were independently performed at least three times. **f** Relative fungal biomass in infected alfalfa tissues. The relative fungal biomass was determined by qPCR analysis as ratios of *FpITS* (as a fungal growth indicator)/alfalfa *MsRBL* (as a host internal reference). Data shown are means + SD, and asterisks indicate the significant difference (*t*-test, $^*P < 0.05$)

Table S3). Notably, these 24 putative virulence-associated genes exhibited distinctive expression patterns during infection *in planta* (Fig. 5c). Collectively, the RNA-seq findings imply that the deletion of *FpOGT* not only disrupted RNA metabolism and ribosome functioning but also influenced intricately the expression of pathogenic-related genes.

FpOGT regulates the expression of virulence-related protein FpGCK by influencing its expression levels

As RNA-Seq can also provide data on alternative splicing, we further analyzed differential transcripts and alternative splicing in Δ*FpOGT*. Data revealed the presence of mutually exclusive alternative splicing in a putative glucokinase gene *FpGCK* (*FPRO_09769*). Specifically, the second and third exons of *FpGCK* exhibit a mutually exclusive pattern, giving rise to two distinct isoforms termed *FpGCK*-AS1 and *FpGCK*-AS2 (Fig. 6a). Intriguingly, in Δ*FpOGT*, the abundance of the *FpGCK*-AS1 isoform was significantly reduced, indicating that the disruption of *FpOGT* influences the transcript levels of *FpGCK*-AS1 (Fig. 6b). This finding was further validated by RT-PCR, which consistently demonstrated a marked reduction in the expression of *FpGCK*-AS1 in Δ*FpOGT* (Fig. 6c). Subsequent investigations at the protein level also showed a significant decrease in the expression of

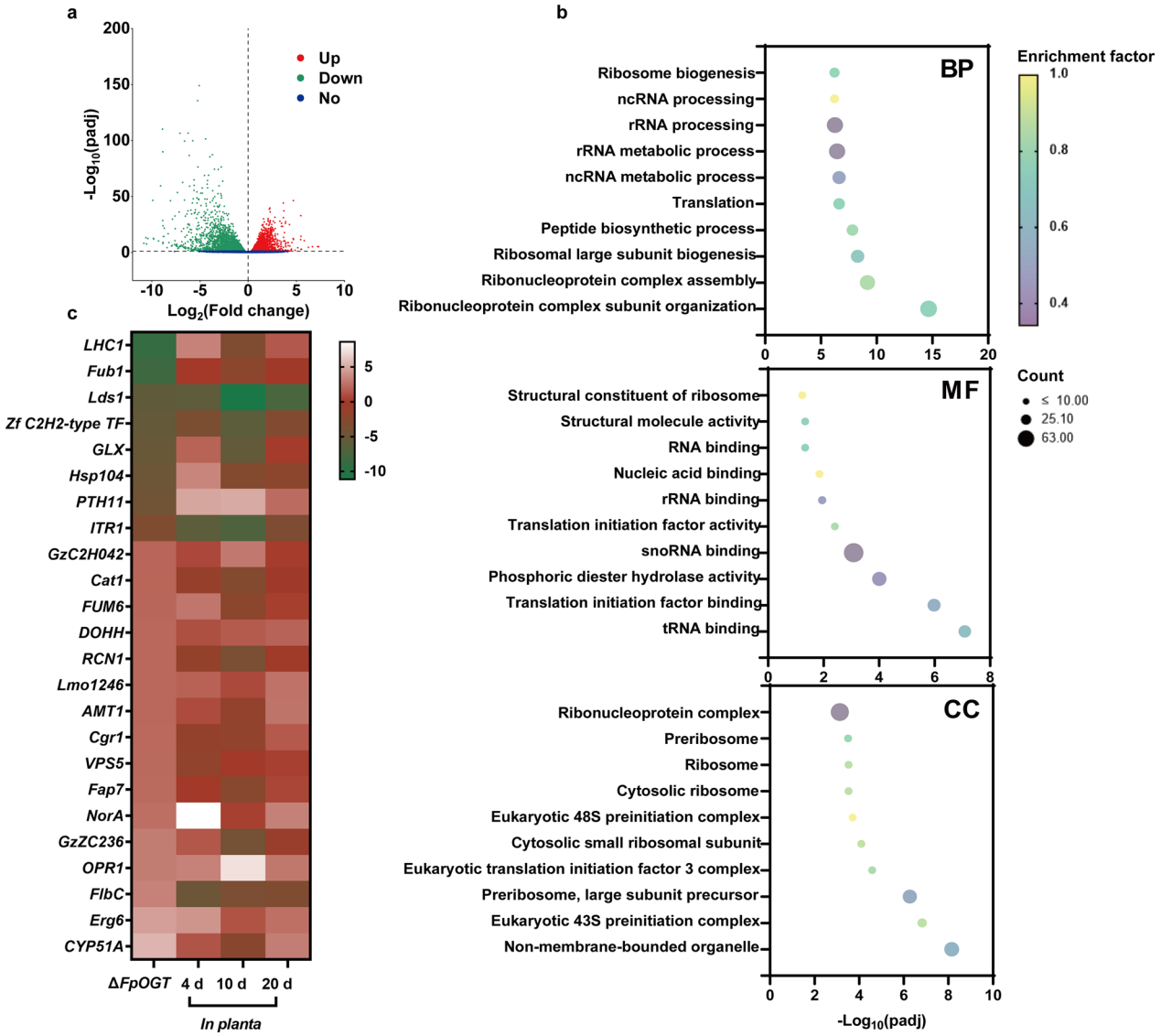

Fig. 5 FpOGT modulates the expression of genes involved in RNA metabolism, ribosome metabolism, and virulence-related processes in *Fp*. **a** Volcano map of differential expression genes in Δ*FpOGT*. Up-regulated genes (Up) are shown by red dots, down-regulated genes (Down) by green dots, while unchanged genes (No) are marked as blue dots. **b** Bubble map of GO enrichment analysis. BP, biological progress; MF, molecular function; CC, cellular component. The bubble color indicates the enrichment factor and the bubble size indicates the number of genes. **c** Heat map of the expression of putative virulence-related genes in Δ*FpOGT* or during plant infection

FpGCK-AS1-GFP protein in Δ*FpOGT* compared to the WT background (Fig. 6d). This observation suggests that FpOGT modulates the protein abundance of FpGCK by regulating the transcript levels of the *FpGCK*-AS1, consequently influencing the function of FpGCK. To ascertain the impact of this regulation on *Fp* virulence, we knocked out *FpGCK* and determined the virulence of Δ*FpGCK* mutant. Results showed that the virulence of the Δ*FpGCK* strain was slightly decreased (Fig. 6e, f), implying that *FpGCK* is involved in the *FpOGT*-mediated virulence in *Fp*.

Molecular docking assay suggested a potential binding between FpOGT and FpGCK

Previous studies revealed that O-GlcNAcylation plays a role in modulating the stability of glucokinase in mice liver. Specifically, the siRNA-induced reduction of OGT resulted in decreased GCK protein levels and its O-GlcNAcylation levels (Baldini et al. 2016). Hence, we speculated that FpGCK might also serve as a substrate for FpOGT, and O-GlcNAcylation of FpOGT may improve its stability. To test this hypothesis, we investigated their interaction by molecular docking analysis.

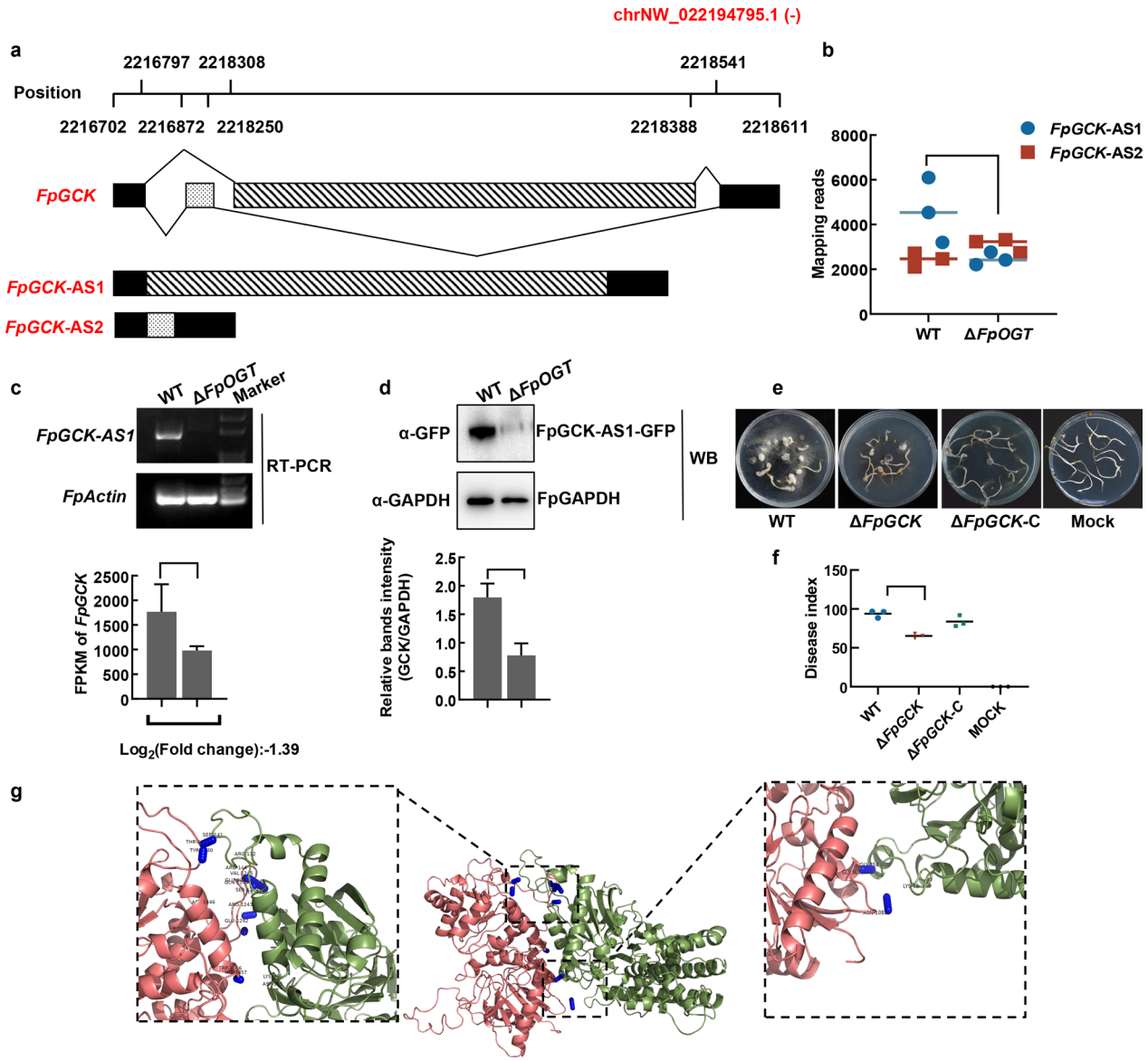

Fig. 6 FpOGT influences the alternative splicing of *FpGCK*-AS1 and thus regulates its expression levels. **a** A simplified model for mutual exclusivity splicing of *FpGCK*. The numbers above the graph indicate the location of each exon of *FpGCK* on the chromosome. **b** RNA-seq reads mapping to *FpGCK*-AS1 and *FpGCK*-AS2 isoform. **c** The expression level of *FpGCK*-AS1 in WT or Δ*FpOGT* detected with RT-PCR (top) and RNA-seq analyses (bottom). **d** Quantification of FpGCK-AS1-GFP expression in WT and Δ*FpOGT* strains by western blot analysis (top). Relative band intensity was normalized to FpGAPDH (bottom). Uncropped gels and blots in c and d are shown in Additional file 2: Figure S7. **e** and **d** Disease phenotype and disease index of the WT-, Δ*FpGCK*-, Δ*FpGCK*-C-inoculated alfalfa seeds. Asterisks indicate a significant difference (*t*-test, $^{*}P < 0.05$). **g** Molecular docking graph of the interaction between FpOGT and FpGCK. Pink, FpOGT model; Green, FpGCK model. Enlarged graphs next to the docking model show the hydrogen bonds interaction with blue bars

The predicted tertiary structures of the FpOGT and FpGCK proteins were obtained and exported in protein data bank (pdb) format. The ZDOCK module of Discovery Studio software was used to perform the docking of FpOGT to the FpGCK protein (Fig. 6g). Subsequently, using the generated docking models, we analyzed the FpOGT and FpGCK interfaces employing the PDBePISA resource (Additional file 2: Figure S5a). We have designated our docking models as Structure 1 (FpOGT) and 2 (FpGCK), and detailed statistics for the interface calculation of the docking results are presented in Additional file 2: Figure S5b. In the docking model, hydrogen bond interactions were observed with specific amino acid residues, such as 1:THR1431:N-2:SER141:O, 1:

TYR1430:OH-2:ARG144:O, 1:SER1244:OG-2:HIS147:O, 1:SER1244:OG-2:ILE148:N, and other amino acid sites (Additional file 2: Figure S5b). The optimal docking results were visualized using Pymol, and a comprehensive analysis indicated the formation of a stable protein docking model between FpOGT and FpGCK (Additional file 2: Figure S5c), suggesting that FpOGT may interact directly with FpGCK to form a functional complex.

FpOGT modulates glucose metabolism-related processes in *Fp*

Glucokinase is a key enzyme in glucose metabolism (Ren et al. 2022). O-GlcNAcylation is thought to act as a nutrient sensor that regulates cellular processes based on nutrients (Yang and Qian 2017). Therefore, we hypothesized that FpOGT might play a role in modulating glucose metabolism in *Fp*. To investigate this, we analyzed the expression of key genes involved in glycolysis, TCA cycle, and HBP pathway in Δ*FpOGT*. Results revealed differential expression of most key enzymes in these pathways in Δ*FpOGT* (Fig. 7a, b and Additional file 1: Table S4). Additionally, DEGs in Δ*FpOGT* have also been enriched in glucose metabolism-related KEGG pathways, including glycolysis, pyruvate metabolism, carbon metabolism, and citrate cycle (Fig. 7c). Taken together, these results indicate that disruption of FpOGT significantly alters the expression of genes encoding enzymes participating in glycolysis, the TCA cycle, and the HBP pathway, ultimately resulting in defects in mycelial growth and pathogenicity of *Fp*.

The role of FpOGT in regulating glucose metabolism is closely related to FpGCK

Previous experiments have demonstrated that knocking out *FpOGT* has an impact on the levels of FpGCK protein, and the regulatory role of FpOGT in glucose metabolism is evident (Fig. 7). To further elucidate the relationship between FpOGT and FpGCK in the regulation of glucose metabolism, we generated the Δ*FpOGT*::FpGCK-GFP strain overexpressing FpGCK in the Δ*FpOGT* mutant background. Results of the growth assay showed that the overexpression of FpGCK could partially restore the growth defects of Δ*FpOGT* (Fig. 8a). Meanwhile, the disease assay also showed that the virulence of Δ*FpOGT*:: FpGCK-GFP strain was increased although not fully restored to the WT level (Fig. 8b, c). These results suggest that the deficiency in growth and virulence of the Δ*FpOGT* strain is associated with the reduced abundance of FpGCK. Additionally, we assessed the expression levels of several key genes involved in glycolysis and the TCA cycle in the Δ*FpOGT*:: FpGCK-GFP strain. The results demonstrated that a subset of these genes were up-regulated in the Δ*FpOGT*:: FpGCK-GFP strain compared to Δ*FpOGT* strain (Fig. 8d). Besides, we also observed that the FpGCK-GFP fusion protein colocalized with the mitochondrial marker Mito-Tracker, suggesting that FpGCK is distributed within mitochondria (Fig. 8e, f). Overall, FpOGT regulates glucose metabolism in a manner similar to FpGCK, as indicated by these results.

Discussion

O-GlcNAcylation, an indispensable post-translational modification of proteins, influences protein expression, stability, and turnover (Yang and Qian 2017). Despite its significance, the regulation of OGT remains intricate and not fully comprehended. Recent studies have shed light on the wide distribution of O-GlcNAc on nuclear, mitochondrial, and cytoplasmic proteins, encompassing well-studied entities like RNA polymerase II, histones, and ribosomal proteins (Gurel et al. 2014). Beyond this, O-GlcNAcylation plays a vital role in the regulation of numerous cellular processes, with its involvement in cell metabolism being an emerging area of investigation (Machacek et al. 2018). However, the investigation of O-GlcNAcylation in fungi has been limited. To examine the occurrence of O-GlcNAcylation in fungi, we used the HMMER search tool to query 48 fungal protein databases for proteins containing the Glyco_transf_41 domain, which is known to facilitate the addition of O-GlcNAc to serine and threonine residues (Martinez-Fleites et al. 2008). This research enhances our comprehension of the distribution of O-GlcNAcylation and its potential implications on various biological processes in diverse organisms. O-GlcNAcylation is a distinctive form of glycosylation observed in eukaryotes, such as *C. elegans*, humans, and plants (Hart et al. 2011). These organisms possess O-GlcNAc transferases that are highly conserved, whereas O-GlcNAcylation has not yet been documented to occur in prokaryotes and budding yeast (Hart et al. 2011). In this investigation, we performed an extensive bioinformatics analysis on protein databases of 48 fungi, which led to the identification of a single OGT in 38 filamentous fungi (Additional file 1: Table S1). Remarkably, we also discovered the presence of an OGT protein in *Yarrowia lipolytica*, which can be attributed to its evolutionary proximity to filamentous fungi rather than its distant relationship with *Saccharomyces cerevisiae* and *Candida albicans* (Fig. 1a and Additional file 1: Table S1). The examination of the domain architecture, conserved motifs, and physicochemical properties of OGT proteins in the 38 filamentous fungi reveals the conservation of both structure and function (Fig. 1b, c and Additional file 2: Figure S1). Particularly, the OGT proteins in the six species of

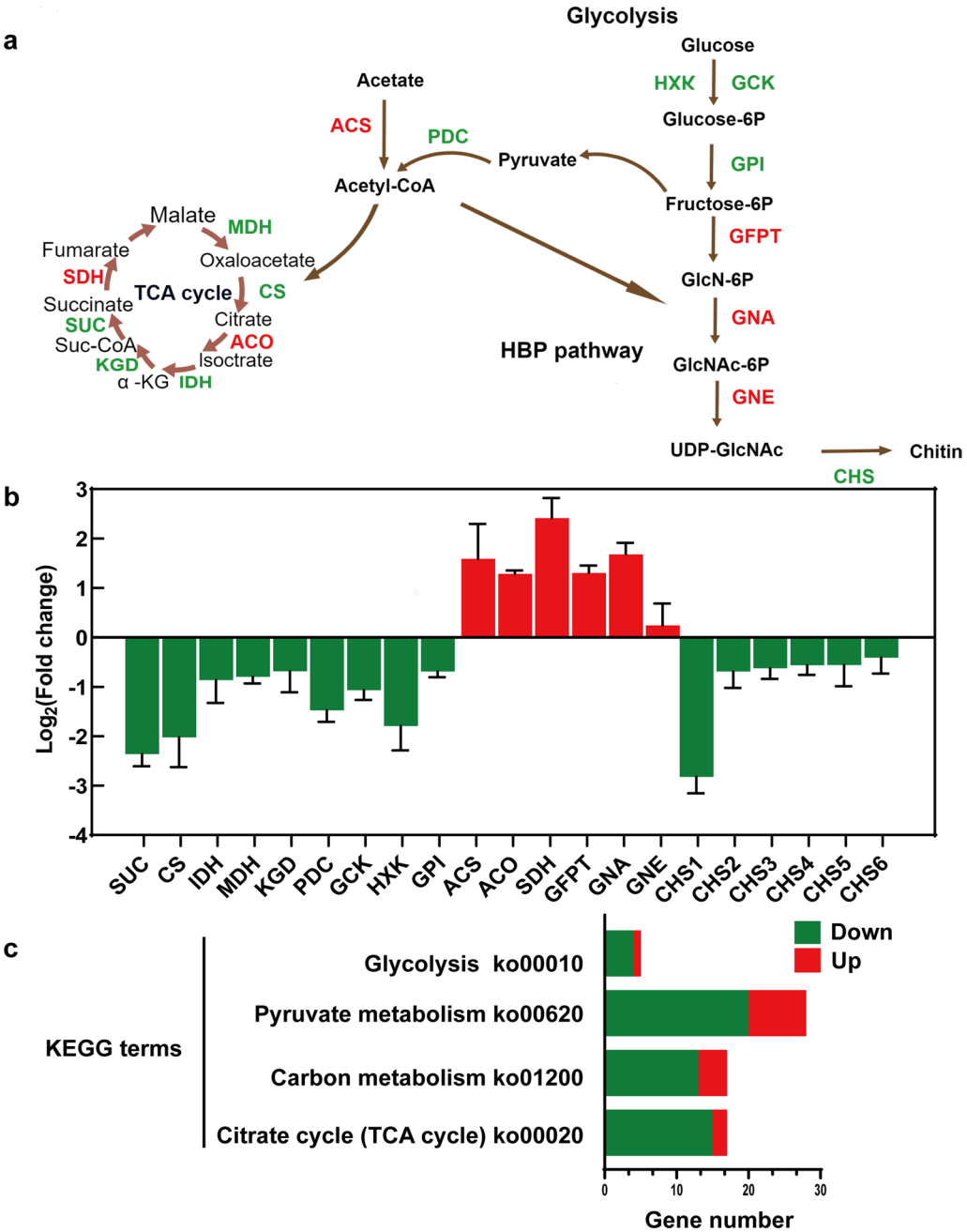

Fig. 7 FpOGT regulates the expression of genes involved in glucose metabolism-related processes in *Fp*. **a** A diagram showing DEGs in the TCA cycle, Glycolysis, HBP pathway, and Chitin synthesis. The red font indicates up-regulated genes. Green font indicates down-regulated genes. **b** Expression fold change of the *SUC*, *CS*, *ACS*, *PDC*, *GCK*, *PDC2*, *IDH*, *PDC3*, *MDH*, *GPI*, *KGD*, *HXK*, *GNE*, *ACO*, *GFPT*, *ACS1*, *GNA*, *SDH*, *CHS1*, *CHS2*, *CHS3*, *CHS4*, *CHS5*, *CHS6* genes. **c** KEGG enrichment terms of DEGs involved in glucose metabolism-related processes

Fusarium display significant resemblance in secondary and tertiary structures, indicating the preservation of their functional structures (Additional file 2: Figure S2). Consequently, our study on FpOGT holds reference value for exploring O-GlcNAcylation in *Fusarium* spp. and potentially other phytopathogenic fungi.

The biological significance of O-GlcNAcylation is well-documented, with its involvement in diverse cellular processes. In *Drosophila*, O-GlcNAcylation has been associated with the wing vein phenotype and developmental lethality (Martinez-Fleites et al. 2008). Similarly, our study on *FpOGT* deletion mutant revealed defects

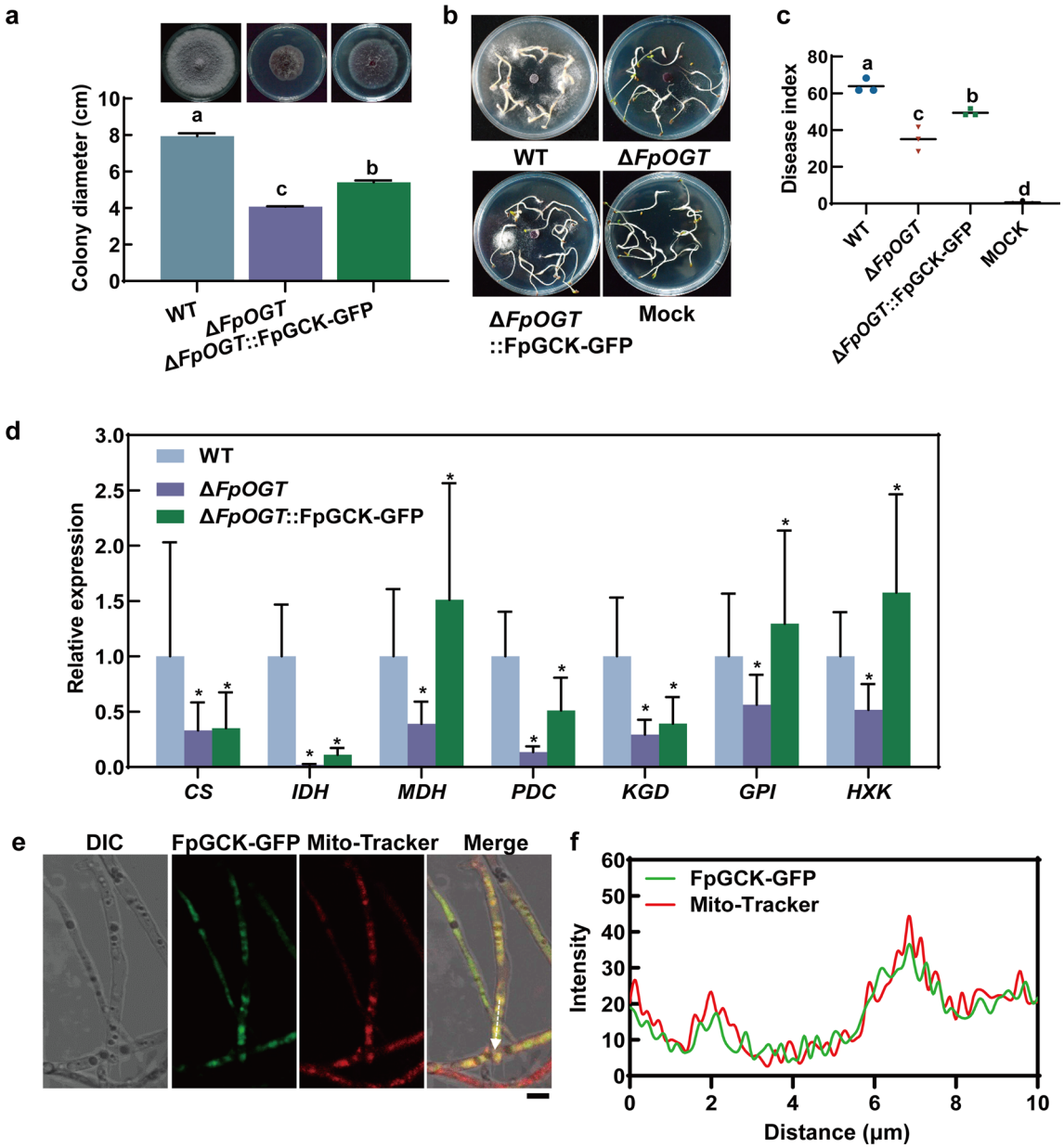

Fig. 8 Overexpression of FpGCK partially restores the defects of Δ*FpOGT* in growth, virulence, and glucose metabolism. **a** Colony growth and diameters of WT, Δ*FpOGT,* and Δ*FpOGT*::FpGCK-GFP grown on PDA at 28 °C for 7 d. **b** and **c** Disease phenotypes and disease index of the WT-, Δ*FpOGT*-, Δ*FpOGT*::FpGCK-GFP-inoculated alfalfa seeds. **d** Relative expression of genes encoding key enzymes in glucose metabolism in WT, Δ*FpOGT*, and Δ*FpOGT*::FpGCK-GFP strains. Relative expression is normalized to *FpActin*. **e** FpGCK-GFP and Mito-Tracker fluorescence signals. White arrows indicate linescan graph analysis areas. Scale bars: 5 μm. **f** Linescan graphs showing the colocalization of fluorescence signals from FpGCK-GFP and Mito-Tracker. Data shown are means + SD. Asterisks indicate the significant difference compared with WT strain (*t*-test, $^*P < 0.05$)

in mycelial growth and macroconidia morphology in *Fp* (Fig. 2c–e). In addition, O-GlcNAcylation is critical for cellular survival during cellular stress responses, affecting metabolism, transcription, translation, and signal transduction (Ma et al. 2021). Previous research has demonstrated its effects in various stress conditions, including heat shock, oxidative stress, ethanol stress, genotoxic stress, reductive stress, endoplasmic reticulum stress, and osmotic stress (Urso et al. 2020; Fahie et al. 2022). In line with these findings, our study indicated that the deletion of *FpOGT* in *Fp* significantly affected sensitivity to the cell wall, osmotic, and metal

ion stresses (Fig. 3a, b). Beyond its implications in cellular physiology, aberrant O-GlcNAcylation has been linked to human disorders like diabetes, cancer, neurodegenerative, and cardiovascular diseases, leading to a growing interest in targeting O-GlcNAcylation for therapeutic interventions (Lin et al. 2021). Our research demonstrates that FpOGT plays a role in various essential physiological processes of *Fp*, such as mycelial growth, conidia morphogenesis, response to environmental stress, and pathogenicity (Figs. 2, 3, 4). This role is achieved by regulating the expression of different groups of genes, particularly those related to glucose metabolism (Figs. 5, 7). However, the underlying mechanisms by which FpOGT regulates specific biological processes remain to be elucidated, necessitating the characterization of O-GlcNAcylated substrates for FpOGT.

O-GlcNAcylation exerts a significant influence on glucose metabolism and nutrient sensing in response to environmental changes and physiological signals, assuming the roles of both a "stress receptor" and "nutrition sensor" in various stress responses and biological processes (Sun et al. 2016; Peng et al. 2017; Sodi et al. 2018). This post-translational modification critically regulates the structure and function of numerous metabolic enzymes, presenting a vital mechanism for cellular metabolic regulation (Zhao et al. 2016). Specifically, the disruption of *FpOGT* resulted in a significant reduction in the abundance of the *FpGCK*-AS1 isoform, indicating that FpOGT indeed plays a crucial role in regulating the expression level of *FpGCK* (Fig. 6a–d). This observation aligns with the outcomes of experiments conducted by other researchers, where O-GlcNAcylation was found to regulate the stability of glucokinase in the liver of mice, and siRNA-mediated knockdown of *OGT* led to decreased O-GlcNAc and GCK protein levels (Baldini et al. 2016). Furthermore, we propose a potential direct interaction between FpOGT and FpGCK, forming a functional complex that likely contributes to the observed regulatory outcomes (Fig. 6g and Additional file 2: Figure S5). However, this needs to be confirmed by further experimental studies. Besides, the disruption of *FpOGT* led to significant alterations in the expression of key enzymes involved in glycolysis, the TCA, and the HBP pathway (Fig. 7). These findings are in accord with previous studies that highlight the pivotal role of O-GlcNAcylation in coordinating glycolysis and the TCA cycle, thereby influencing cell proliferation and tumorigenesis (Sun et al. 2016; Nie et al. 2020). Above all, these discoveries not only advance our understanding of the molecular mechanisms underlying *Fp* virulence but also highlight the significance of O-GlcNAcylation in governing essential cellular processes, with implications for the broader field of fungal pathogenesis and metabolic regulation.

The results of our study provide evidence supporting the role of FpOGT in the regulation of multiple aspects of *Fp* such as mycelial growth, spore morphogenesis, responses to abiotic stress and fungicide treatment, and its influence on virulence. The results obtained from the experiments provide significant insights into the intricate relationship between FpOGT and FpGCK, unraveling their collaborative influence on glucose metabolism. The observed impact of *FpOGT* knockout on FpGCK protein levels, coupled with the evident regulatory role of FpOGT in glucose metabolism, prompted our deeper investigation. Our subsequent findings suggest that overexpression of FpGCK in Δ*FpOGT* partially restores the growth defects, as demonstrated in Fig. 8a. While the Δ*FpOGT*::FpGCK-GFP strain exhibited increased virulence compared to Δ*FpOGT*, it did not fully restore to the wild-type level (Fig. 8b, c). Moreover, the expression of several genes involved in glycolysis and TCA cycle in the Δ*FpOGT*::FpGCK-GFP strain was up-regulated compared to Δ*FpOGT* (Fig. 8d). These results collectively indicate that the impact of FpOGT on glucose metabolism is associated with its regulatory influence on FpGCK. We suggest that this influence is likely indirect, and the intrinsic relationship can be elucidated by considering FpGCK as a potential modification substrate for FpOGT. The O-GlcNAc modification of FpGCK may affect its stability.

In summary, we proposed that FpOGT may interact with FpGCK and potentially mediate the O-GlcNAc modification of FpGCK, thereby regulating the level of *FpGCK*-AS1 transcript isoform. In addition, O-GlcNAcylation of FpGCK may affect its stability by avoiding degradation. This regulation, in turn, modulates glucose metabolic processes in mitochondria, such as glycolysis, the tricarboxylic acid cycle, and the hexosamine biosynthesis pathway, ultimately influencing the virulence of *Fp* (Additional file 2: Figure S6). This extensive inquiry not only provides insights into the role of O-GlcNAcylation in fungi but also enhances our comprehension of the molecular mechanisms underlying the virulence of *Fp*. Moreover, our findings can contribute to a better understanding of the O-GlcNAcylation mechanism in other species.

Conclusion

Our research has elucidated the significant influence of FpOGT as a regulator of vegetative growth, tolerance to environmental stress, and virulence in *F. proliferatum*. The deletion of FpOGT also impacts the expression levels of FpGCK, thereby influencing glucokinase function, regulating glucose metabolism, mitochondrial metabolism,

and other related pathways. The molecular docking results provide additional evidence to support the potential physical interaction between FpOGT and FpGCK. These findings contribute to a deeper understanding of the complex mechanisms involved in the development and virulence of *F. proliferatum*.

Methods

Fungal strains and culture conditions

Fusarium proliferatum strain HM19-1-1 was used as the wild-type strain for gene deletion mutant construction and fungal transformation (Wang et al. 2023). *Fp* strains were cultured on potato dextrose agar (PDA) for mycelial growth assays. Sporulation analysis was performed in carboxymethyl cellulose (CMC) liquid medium.

Bioinformatics analyses

OGT sequence searches among fungi protein databases were performed using the HMMER tool (http://hmmer.org/). Conserved motif of OGT proteins was analyzed using MEME (https://meme-suite.org/meme/tools/meme). The phylogenetic tree was constructed for OGT proteins using TBtools (Chen et al. 2020). The physicochemical properties of the predicted fungi OGT proteins were analyzed using the Expasy ProtParam tool (https://web.expasy.org/protparam/). The analysis included the determination of protein length and isoelectric point of the OGT proteins. A total of 38 fungi species were categorized based on their lifestyle, and using GraphPad Prism 9.5, violin plots were constructed to visualize the protein length and isoelectric point of OGT proteins for each lifestyle category. Protein secondary structure was predicted using the NPS@SOPMA (https://npsa.lyon.inserm.fr/cgi_bin/npsa_automat.pl?page=/NPSA/npsa_sopma.html). Protein tertiary structure was predicted by SWISS-MODEL (http://swissmodel.expasy.org/) using the default parameters. Subsequently, the predicted protein tertiary structures were subjected to visualization using PyMOL software.

Construction of gene deletion mutants and strains for complementation test

Fusion PCR product, comprising the upstream fragment, *HPH* cassette, and downstream fragment, was achieved through three PCR steps with gene-specific primers (Additional file 1: Table S2). Subsequently, the obtained double-joint cassette was transformed into WT protoplasts. The transformed protoplasts were screened on PDA medium containing 100 mg/mL hygromycin B to identify potential deletion transformants. Potential transformants were further verified using PCR with identification primers (Additional file 1: Table S2). Additionally, the copy number of the double-joint cassette in putative transformants was analyzed by Southern blotting (Xu et al. 2023b). The DNA fragment encoding the truncated FpOGT protein spanning residues 428 to 1491, including the TPR and Glyco domains, was cloned, with an initiating codon ATG appended to the end of the forward primers. Subsequently, a double-joint PCR method was used to fuse this DNA fragment with the RP27 promoter, mCherry fragment, and G418 resistance gene fragment. Then, the fused RP27-mcherry-FpOGT-TV-G418 fragment was transformed into Δ*FpOGT* protoplasts. PCR and qPCR methods were used to verify transformants selected from the PDA containing 50 μg/mL G418.

Growth, conidiation, and stress-sensitivity tests

The mycelial growth and colony morphology of WT and Δ*FpOGT* strains were assessed on PDA plates at 28°C for 7 d. For the conidiation assay, each strain was cultured in CMC broth at 28°C and subjected to shaking at 200 rpm for 3 d before the number of conidia was counted. To visualize and count the conidia, the OLYMPUS IX73 microscope was used. Stress tolerance experiments were carried out by cultivating the strains on PDA plates supplemented with various stress-inducing agents, including 0.2% congo red, 0.2% calcofluor white, 0.05% sodium dodecyl sulfate, 2 M sodium chloride, 1.4 M calcium chloride, 0.05% chlorothalonil, 0.05% metalaxyl, 0.2% *Bacillus subtilis*, or 0.2% fludioxonil, for 7 d. The assessment of stress sensitivity was based on the determination of the growth inhibition rate (Qu et al. 2022).

Fungal virulence assay

A culture plate method was used for the virulence assay (Berg et al. 2017). *Fp* strains were cultured on the 1% water agar (WA) plate at 28°C for 5 d. After disinfecting the alfalfa seeds with 70% ethanol for 1 min and three times rinsing with sterile water, they were subjected to an 8% sodium hypochlorite solution for 1 min and rinsed three times with sterile water. Subsequently, 15–20 seeds were evenly distributed on the aforementioned WA plates with the cultured *Fp* colony, while WA plates without *Fp* were used as the mock control. Each treatment had three replicates, and after incubating at 28°C for 10 d, the occurrence and severity of the disease were investigated and graded according to disease severity standards. The disease index was assessed using a 0 to 3 rating scale: Grade 1 indicates yellowing and softening of the root tips; Grade 2 signifies severe browning and rotting of the seedlings; Grade 3 denotes non-germinated seeds enwrapped with mycelia. The infected seeds and seedlings were collected for fungal growth assay. Fungal biomass in seeds or seedlings was calculated by qPCR via normalizing the DNA levels of *FpITS* and alfalfa *MsRBL*. For seedlings inoculation, the virulence assay was performed on

3-week-old alfalfa seedlings using the root dipping inoculation method (Wang et al. 2023). Thirty days after inoculation, the survival rates of all seedlings were determined.

RNA isolation and qRT-PCR

Total RNA was isolated using the RNA isolator reagent (Vazyme, Nanjing, China) following the manufacturer's instructions, and then cDNA was obtained using the HiScript III First Strand cDNA Synthesis Kit (Vazyme, Nanjing, China). Real-time analysis was performed using the Applied Biosystems 7500 machine (Thermo Fisher Scientific, Waltham, USA), and amplification was performed using ChamQ SYBR qPCR Master Mix (Vazyme, Nanjing, China). The primer sequences used for the qRT-PCR (quantitative real-time PCR) assays can be found in Additional file 1: Table S2. The $2^{-\Delta\Delta CT}$ method was employed to assess the relative expression level of genes, with the *FpActin* (*FPRO_04359*) as the reference gene.

RNA sequencing

RNA sequencing was performed by Applied Protein Technology (Shanghai, China). Firstly, the WT and Δ*FpOGT* strains were cultured on potato dextrose broth (PDB) at 28°C for 3 d, and the mycelia were swiftly collected and cryogenically preserved in liquid nitrogen. Subsequently, total RNA was extracted for the construction of the RNA library. Raw data quality assessment was performed by FastQC. TopHat2 software was used to map clean reads to the reference genome of *Fp* ET1 (Kim et al. 2013). Gene expression was standardized as fragments per kilobase per million (FPKM) in the RSEM program (Li and Dewey 2011). DEGs were analyzed using the DESeq2 package. The GO and KEGG pathway enrichment analysis of DEGs using ClusterProfiler R. The differential alternative splicing (AS) events between the WT and Δ*FpOGT* groups were compared using the rMATS tool (http://rnaseq-mats.sourceforge.net/index.html).

Western blot

Western blot analysis was conducted following the established method (Huang et al. 2023). Briefly, mycelia were collected, washed, and lysed in RIPA lysis buffer (Beyotime, Shanghai, China) supplemented with protease inhibitors phenylmethylsulfonyl fluoride and complete protease inhibitor cocktail (Roche Diagnostics, Mannheim, Germany). The proteins were transferred to the polyvinylidene difluoride membrane after 12.5% SDS-PAGE separation. Immunoblotting was performed at 4°C overnight after blocking the membranes for an hour at room temperature. Horseradish peroxidase-conjugated secondary antibody (Beyotime, Shanghai, China) was then added to the membranes. Immunoreactive protein signal was detected using the Immobilon Western reagent (Merck Millipore, Darmstadt, Germany), and imaging was visualized using the Omega Lum C system (Aplegen, San Francisco, USA).

Molecular docking

The molecular docking of FpOGT with FpGCK was performed following the previous method (Moreira et al. 2010). Using SWISS-MODEL, we predicted the tertiary structures of proteins, which were then exported in pdb format. A coarse-grained search for the interaction of FpOGT and FpGCK was performed using the protein-protein docking method ZDOCK (http://zdock.umassmed.edu/). The docked complex structure model was further analyzed in the PDBePISA resource and then visualized in Pymol.

Microscopic examinations

Fresh mycelia were examined using a Zeiss LSM780 confocal microscope (Carl Zeiss AG, Oberkochen, Germany) to visualize fluorescence signals of FpGCK-GFP and Mito-Tracker Red CMXRos (Beyotime Biotechnology, Nantong, China). The Mito-Tracker Red fluorescence was observed through the rhodamine filter set (excitation 585 nm, emission 624 nm), while the FpGCK-GFP signal was captured using the GFP filter set (excitation 488 nm, emission 520 nm). Colocalization analyses were performed using ImageJ software to assess the degree of overlap between the two fluorescence signals.

Abbreviations

AS	Alternative splicing
CFW	Calcofluor white
CMC	Carboxymethyl cellulose
CR	Congo red
DEGs	Differentially expressed genes
Fp	*Fusarium proliferatum*
FPKM	Fragments per kilobase per million
GCK	Glucokinase
GFP	Green fluorescent protein
GO	Gene Ontology
HBP	Hexosamine biosynthesis pathway
HPH	Hygromycin phosphotransferase
KEGG	Kyoto Encyclopedia of Genes and Genomes
MM	Minimal medium
OGA	O-GlcNAcase
OGT	O-GlcNAc transferase
PDA	Potato dextrose agar
PDB	Potato dextrose broth
pdb	Protein data bank
PHI-base	Pathogen-host interactions database
PTMs	Post-translational modifications
qRT-PCR	Quantitative real-time PCR
RNA-seq	RNA sequencing
SDS	Sodium dodecyl sulfate
TCA	Tricarboxylic acid
TPR	Tetratricopeptide repeat
UDP-GlcNAc	Uridin diphosphate N-acetylglucosamine
WA	Water agar

Supplementary Information

The online version contains supplementary material available at https://doi.org/10.1186/s42483-023-00221-w.

Additional file 1: **Table S1**. OGT proteins in fungi. **Table S2**. Primers used in the paper. **Table S3**. Putative virulence-related genes regulated by FpOGT. **Table S4**. Gene ID list in Fig.7.

Additional file 2: **Figure S1**. Distribution of the conserved motif of OGT proteins in fungi. **Figure S2**. Secondary structures and tertiary structure model graphs of OGT proteins in *Fusarium* spp. **a** Percentage of the secondary structures of the OGT proteins. **b** Predicted tertiary structures of OGT proteins in *Fusarium* spp. using the SWISS-MODEL server. **c** Comparison analysis and quality evaluation on the tertiary structures of OGT from *Fusarium* spp. **Figure S3**. Validation of FpOGT gene knockout transformants and truncated complemented transformants. **a** Schematic diagram of FpOGT-targeted knockout strategy. Green and red bars are the primers used in PCR identification. Blue bar, the probes used in Southern analysis. **b** PCR identification of the FpOGT-knockout mutants. **c** Southern blotting of the FpOGT-targeted disruption strains. **d** PCR validation of the ΔFpOGT-TV-C strains. **e** Expression of FpOGT gene in WT, knockout strain, and complemented strain. W, wild type; M, mutant; Ec, ectopic transformant; C, complemented transformants; P, positive control. Uncropped gel images are shown in Additional file 1: Figure S6. **Figure S4**. Phenotypes of FpOGT gene knockout transformants and ectopic transformants. **a** Disease phenotypes of alfalfa seedlings inoculated by WT, FpOGT knockout transformants, and ectopic transformants. **b** Disease ratings and **c** Disease index of the inoculated seedlings of WT, FpOGT knockout transformants, and ectopic transformants at 10 dpi. **d** Colony growth of WT, *FpOGT* knockout transformants, and ectopic transformants on PDA plates. **Figure S5**. FpOGT-FpGCK docking structures and their interface interactions. **a** FpOGT(left)-FpGCK(right) docking and interface graph. **b** Hydrogen bond interactions observed in the docking model. **c** FpOGT-FpGCK interface description from the PDBePISA resource. **Figure S6**. A proposed working model for the mechanism of the FpOGT-FpGCK module in *Fp*. **Figure S7**. Uncropped gels and blots images.

Acknowledgements
We thank Dr. Yuanyuan Zhang (Institute of Grassland Research of the Chinese Academy of Agricultural Sciences) for providing the HM19-1-1 strain.

Author contributions
YZ, YT, SM, and ZH designed experiments; YZ, YT, SM, HB, and JW performed the experiments; YZ, YT, SM, and ZH analyzed the data; YZ, YT, and ZH wrote the manuscript. All authors read and approved the final manuscript.

Funding
This work was supported by the Scientific Research Foundation of Zhejiang University of Science and Technology (No. F701103M09) and the general scientific research project from the Education Department of Zhejiang Province (Y202351867).

Availability of data and materials
Not applicable.

Declarations

Ethics approval and consent to participate
Not applicable.

Consent for publication
Not applicable.

Competing interests
The authors declare that they have no competing interests.

Received: 31 July 2023 Accepted: 23 December 2023
Published online: 11 January 2024

References

Abbas A, Mubeen M, Sohail MA, Solanki MK, Hussain B, Nosheen S, et al. Root rot a silent alfalfa killer in China: distribution, fungal, and oomycete pathogens, impact of climatic factors and its management. Front Microbiol. 2022;13: 961794. https://doi.org/10.3389/fmicb.2022.961794.

Baldini SF, Steenackers A, Olivier-Van Stichelen S, Mir AM, Mortuaire M, Lefebvre T, et al. Glucokinase expression is regulated by glucose through O-GlcNAc glycosylation. Biochem Biophys Res Commun. 2016;478:942–8. https://doi.org/10.1016/j.bbrc.2016.08.056.

Berg LE, Miller SS, Dornbusch MR, Samac DA. Seed rot and damping-off of alfalfa in Minnesota caused by *Pythium* and *Fusarium* Species. Plant Dis. 2017;101:1860–7. https://doi.org/10.1094/PDIS-02-17-0185-RE.

Bergdahl B, Sandstrom AG, Borgstrom C, Boonyawan T, van Niel EW, Gorwa-Grauslund MF. Engineering yeast hexokinase 2 for improved tolerance toward xylose-induced inactivation. PLoS ONE. 2013;8: e75055. https://doi.org/10.1371/journal.pone.0075055.

Bond MR, Ghosh SK, Wang P, Hanover JA. Conserved nutrient sensor O-GlcNAc transferase is integral to *C. elegans* pathogen-specific immunity. PLoS ONE. 2014;9:e113231. https://doi.org/10.1371/journal.pone.0113231.

Chang YH, Weng CL, Lin KI. O-GlcNAcylation and its role in the immune system. J Biomed Sci. 2020;27:57. https://doi.org/10.1186/s12929-020-00648-9.

Chatham JC, Zhang J, Wende AR. Role of O-Linked N-Acetylglucosamine protein modification in cellular (patho) physiology. Physiol Rev. 2021;101:427–93. https://doi.org/10.1152/physrev.00043.2019.

Chen C, Chen H, Zhang Y, Thomas HR, Frank MH, He Y, et al. TBtools: an integrative toolkit developed for interactive analyses of big biological data. Mol Plant. 2020;13:1194–202. https://doi.org/10.1016/j.molp.2020.06.009.

Cong LL, Sun Y, Kang JM, Li MN, Long RC, Zhang TJ, et al. First report of root rot disease caused by *Fusarium proliferatum* on alfalfa in China. Plant Dis. 2016;100:2526. https://doi.org/10.1094/PDIS-04-11-0307.

D'Andrea LD, Regan L. TPR proteins: the versatile helix. Trends Biochem Sci. 2003;28:655–62. https://doi.org/10.1016/j.tibs.2003.10.007.

Dang SZ, Li YZ. The Characterization and the biological activity of phytotoxin produced by *Paraphoma radicina*. J Fungi (basel). 2022;8:867. https://doi.org/10.3390/jof8080867.

De Backer I, Hussain SS, Bloom SR, Gardiner JV. Insights into the role of neuronal glucokinase. Am J Phys Endocrinol Metab Seoul. 2016;311:E42-55. https://doi.org/10.1152/ajpendo.00034.2016.

Fahie KMM, Papanicolaou KN, Zachara NE. Integration of O-GlcNAc into stress response pathways. Cells. 2022;11:3509. https://doi.org/10.3390/cells11213509.

Gurel Z, Zaro BW, Pratt MR, Sheibani N. Identification of O-GlcNAc modification targets in mouse retinal pericytes: implication of p53 in pathogenesis of diabetic retinopathy. PLoS ONE. 2014;9: e95561. https://doi.org/10.1371/journal.pone.0095561.

Hart GW, Slawson C, Ramirez-Correa G, Lagerlof O. Cross talk between O-GlcNAcylation and phosphorylation: roles in signaling, transcription, and chronic disease. Annu Rev Biochem. 2011;80:825–58. https://doi.org/10.1146/annurev-biochem-060608-102511.

Hu J, Gao QZ, Yang Y, Xia J, Zhang WJ, Chen Y, et al. Hexosamine biosynthetic pathway promotes the antiviral activity of SAMHD1 by enhancing O-GlcNAc transferase-mediated protein O-GlcNAcylation. Theranostics. 2021;11:805–23. https://doi.org/10.7150/thno.50230.

Huang ZL, Lou JJ, Gao YZ, Noman M, Li DY, Song FM. FonTup1 functions in growth, conidiogenesis and pathogenicity of *Fusarium oxysporum* f. sp. niveum through modulating the expression of the tricarboxylic acid cycle genes. Microbiol Res. 2023;272:127389. https://doi.org/10.1016/j.micres.2023.127389.

Joiner CM, Li H, Jiang JY, Walker S. Structural characterization of the O-GlcNAc cycling enzymes: insights into substrate recognition and catalytic mechanisms. Curr Opin Struct Biol. 2019;56:97–106. https://doi.org/10.1016/j.sbi.2018.12.003.

Kim M, Lim JH, Ahn CS, Park K, Kim GT, Kim WT, et al. Mitochondria-associated hexokinases play a role in the control of programmed cell death in

Nicotiana benthamiana. Plant Cell. 2006;18:2341–55. https://doi.org/10.1105/tpc.106.041509.
Kim D, Pertea G, Trapnell C, Pimentel H, Kelley R, Salzberg SL. TopHat2: accurate alignment of transcriptomes in the presence of insertions, deletions and gene fusions. Genome Biol. 2013;14:R36. https://doi.org/10.1186/gb-2013-14-4-r36.
King DT, Males A, Davies GJ, Vocadlo DJ. Molecular mechanisms regulating O-linked N-acetylglucosamine (O-GlcNAc)-processing enzymes. Curr Opin Chem Biol. 2019;53:131–44. https://doi.org/10.1016/j.cbpa.2019.09.001.
Kriegel TM, Kettner K, Rödel G, Sträter N. Regulatory function of hexokinase 2 in glucose signaling in *Saccharomyces cerevisiae*. J Biol Chem. 2016;291:16477. https://doi.org/10.1074/jbc.L116.735514.
Lalak-Kanczugowska J, Witaszak N, Waskiewicz A, Bocianowski J, Stepien L. Plant metabolites affect *Fusarium proliferatum* metabolism and in vitro fumonisin biosynthesis. Int J Mol Sci. 2023;24:3002. https://doi.org/10.3390/ijms24033002.
Lee JB, Pyo KH, Kim HR. Role and function of o-glcnacylation in cancer. Cancers (basel). 2021;13:5365. https://doi.org/10.3390/cancers13215365.
Li B, Dewey CN. RSEM: accurate transcript quantification from RNA-Seq data with or without a reference genome. BMC Bioinform. 2011;12:323. https://doi.org/10.1186/1471-2105-12-323.
Li F, Yang G, Tachikawa H, Shao K, Yang Y, Gao XD, et al. Identification of novel O-GlcNAc transferase substrates using yeast cells expressing OGT. J Gen Appl Microbiol. 2021;67:33–41. https://doi.org/10.2323/jgam.2020.04.002.
Lin CH, Liao CC, Chen MY, Chou TY. Feedback regulation of O-GlcNAc transferase through translation control to maintain intracellular O-GlcNAc homeostasis. Int J Mol Sci. 2021;22:3463. https://doi.org/10.3390/ijms22073463.
Ma JF, Li YX, Hou CY, Wu C. O-GlcNAcAtlas: a database of experimentally identified O-GlcNAc sites and proteins. Glycobiology. 2021;31:719–23. https://doi.org/10.1093/glycob/cwab003.
Machacek M, Slawson C, Fields PE. O-GlcNAc: a novel regulator of immunometabolism. J Bioenerg Biomembr. 2018;50:223–9. https://doi.org/10.1007/s10863-018-9744-1.
Mariappa D, Ferenbach AT, van Aalten DMF. Effects of hypo-O-GlcNAcylation on *Drosophila* development. J Biol Chem. 2018;293:7209–21. https://doi.org/10.1074/jbc.RA118.002580.
Martinez-Fleites C, Macauley MS, He Y, Shen DL, Vocadlo DJ, Davies GJ. Structure of an O-GlcNAc transferase homolog provides insight into intracellular glycosylation. Nat Struct Mol Biol. 2008;15:764–5. https://doi.org/10.1038/nsmb.1443.
Moreira IS, Fernandes PA, Ramos MJ. Protein-protein docking dealing with the unknown. J Comput Chem. 2010;31:317–42. https://doi.org/10.1002/jcc.21276.
Mutanwad KV, Lucyshyn D. Balancing O-GlcNAc and O-fucose in plants. Febs j. 2022;289:3086–92. https://doi.org/10.1111/febs.16038.
Na HJ, Abramowitz LK, Hanover JA. Cytosolic O-GlcNAcylation and PNG1 maintain *Drosophila* gut homeostasis by regulating proliferation and apoptosis. PLoS Genet. 2022;18: e1010128. https://doi.org/10.1371/journal.pgen.1010128.
Nakanishi H, Li F, Han B, Arai S, Gao XD. Yeast cells as an assay system for in vivo O-GlcNAc modification. Biochim Biophys Acta Gen Subj. 2017;1861:1159–67. https://doi.org/10.1016/j.bbagen.2017.03.002.
Nie H, Ju H, Fan J, Shi X, Cheng Y, Cang X, et al. O-GlcNAcylation of PGK1 coordinates glycolysis and TCA cycle to promote tumor growth. Nat Commun. 2020;11:36. https://doi.org/10.1038/s41467-019-13601-8.
Olszewski NE, West CM, Sassi SO, Hartweck LM. O-GlcNAc protein modification in plants: evolution and function. Biochem Biophys Acta. 2010;1800:49–56. https://doi.org/10.1016/j.bbagen.2009.11.016.
Peng C, Zhu Y, Zhang W, Liao Q, Chen Y, Zhao X, et al. Regulation of the Hippo-YAP pathway by glucose sensor o-glcnacylation. Mol Cell. 2017;68:591-604.e5. https://doi.org/10.1016/j.molcel.2017.10.010.
Qu J, Wang Y, Cai M, Liu Y, Gu L, Zhou P, et al. The bZIP transcription factor UvbZIP6 mediates fungal growth, stress response, and false smut formation in *Ustilaginoidea virens*. Phytopathol Res. 2022;4:32. https://doi.org/10.1186/s42483-022-00137-x.
Ren Y, Li L, Wan L, Huang Y, Cao S. Glucokinase as an emerging anti-diabetes target and recent progress in the development of its agonists. J Enzyme Inhib Med Chem. 2022;37:606–15. https://doi.org/10.1080/14756366.2021.2025362.
Sodi VL, Bacigalupa ZA, Ferrer CM, Lee JV, Gocal WA, Mukhopadhyay D, et al. Nutrient sensor O-GlcNAc transferase controls cancer lipid metabolism via SREBP-1 regulation. Oncogene. 2018;37:924–34. https://doi.org/10.1038/onc.2017.395.
Sternisha SM, Miller BG. Molecular and cellular regulation of human glucokinase. Arch Biochem Biophys. 2019;663:199–213. https://doi.org/10.1016/j.abb.2019.01.011.
Sun C, Shang J, Yao Y, Yin X, Liu M, Liu H, et al. O-GlcNAcylation: a bridge between glucose and cell differentiation. J Cell Mol Med. 2016;20:769–81. https://doi.org/10.1111/jcmm.12807.
Sun L, Chen X, Gao J, Zhao Y, Liu L, Hou Y, et al. Effects of disruption of give *FUM* genes on fumonisin biosynthesis and pathogenicity in *Fusarium proliferatum*. Toxins (basel). 2019;11:327. https://doi.org/10.3390/toxins11060327.
Tan W, Jiang P, Zhang W, Hu Z, Lin S, Chen L, et al. Posttranscriptional regulation of de novo lipogenesis by glucose-induced O-GlcNAcylation. Mol Cell. 2021;81:1890-904.e7. https://doi.org/10.1016/j.molcel.2021.02.009.
Urso SJ, Comly M, Hanover JA, Lamitina T. The O-GlcNAc transferase OGT is a conserved and essential regulator of the cellular and organismal response to hypertonic stress. PLoS Genet. 2020;16: e1008821. https://doi.org/10.1371/journal.pgen.1008821.
Wang L, Wang N, Yu J, Wu J, Liu H, Lin K, et al. Identification of pathogens causing alfalfa *Fusarium* root rot in inner Mongolia. China Agron. 2023;13:456. https://doi.org/10.3390/agronomy13020456.
Xing L, Liu Y, Xu S, Xiao J, Wang B, Deng H, et al. *Arabidopsis* O-GlcNAc transferase SEC activates histone methyltransferase ATX1 to regulate flowering. EMBO J. 2018;37:e98115. https://doi.org/10.15252/embj.201798115.
Xu S, Xiao J, Yin F, Guo X, Xing L, Xu Y, et al. The Protein modifications of O-GlcNAcylation and phosphorylation mediate vernalization response for flowering in winter wheat. Plant Physiol. 2019;180:1436–49. https://doi.org/10.1104/pp.19.00081.
Xu J, Huang Z, Du H, Tang M, Fan P, Yu J, et al. SEC1-C3H39 module fine-tunes cold tolerance by mediating its target mRNA degradation in tomato. New Phytol. 2023a;237:870–84. https://doi.org/10.1111/nph.18568.
Xu Z, Luo Z, Xiong D, Gao M, Tian C. A glycoside hydrolase 12 protein from *Cytospora chrysosperma* triggers plant immunity but is not essential to virulence. Phytopathol Res. 2023b;5:32. https://doi.org/10.1186/s42483-023-00187-9.
Yang XY, Qian KV. Protein O-GlcNAcylation: emerging mechanisms and functions. Nat Rev Mol Cell Biol. 2017;18:452–65. https://doi.org/10.1038/nrm.2017.22.
Yang B, Zhao Y, Lu Y, Tao M, Wang Y, Guo Z. First report of alfalfa root rot caused by fusarium commune in China. Plant Dis. 2023;107:580. https://doi.org/10.1094/pdis-06-22-1335-pdn.
Zentella R, Hu J, Hsieh WP, Matsumoto PA, Dawdy A, Barnhill B, et al. O-GlcNAcylation of master growth repressor DELLA by SECRET AGENT modulates multiple signaling pathways in *Arabidopsis*. Genes Dev. 2016;30:164–76. https://doi.org/10.1101/gad.270587.115.
Zhao L, Feng Z, Yang X, Liu J. The regulatory roles of O-GlcNAcylation in mitochondrial homeostasis and metabolic syndrome. Free Radical Res. 2016;50:1080–8. https://doi.org/10.1080/10715762.2016.1239017.